The ISME Journal (2020) 14:1731–1742
https://doi.org/10.1038/s41396-020-0641-3

ARTICLE

High cell densities favor lysogeny: induction of an H20 prophage is repressed by quorum sensing and enhances biofilm formation in *Vibrio anguillarum*

Demeng Tan[1,2,3] · Mads Frederik Hansen[3,4] · Luís Nunes de Carvalho[3] · Henriette Lyng Røder[3] · Mette Burmølle[3] · Mathias Middelboe[3] · Sine Lo Svenningsen[3]

Received: 19 September 2019 / Revised: 17 March 2020 / Accepted: 18 March 2020 / Published online: 9 April 2020

Abstract

Temperate ϕH20-like phages are repeatedly identified at geographically distinct areas as free phage particles or as prophages of the fish pathogen *Vibrio anguillarum*. We studied mutants of a lysogenic isolate of *V. anguillarum* locked in the quorum-sensing regulatory modes of low (Δ*vanT*) and high (Δ*vanO*) cell densities by in-frame deletion of key regulators of the quorum-sensing pathway. Remarkably, we find that induction of the H20-like prophage is controlled by the quorum-sensing state of the host, with an eightfold increase in phage particles per cell in high-cell-density cultures of the quorum-sensing-deficient Δ*vanT* mutant. Comparative studies with prophage-free strains show that biofilm formation is promoted at low cell density and that the H20-like prophage stimulates this behavior. In contrast, the high-cell-density state is associated with reduced prophage induction, increased proteolytic activity, and repression of biofilm. The proteolytic activity may dually function to disperse the biofilm and as a quorum-sensing-mediated antiphage strategy. We demonstrate an intertwined regulation of phage-host interactions and biofilm formation, which is orchestrated by host quorum-sensing signaling, suggesting that increased lysogeny at high cell density is not solely a strategy for phages to piggy-back the successful bacterial hosts but is also a host strategy evolved to take control of the lysis-lysogeny switch to promote host fitness.

Introduction

Viruses of bacteria, bacteriophages (phages), are key components in marine environments as drivers of microbial evolution, mortality, diversity, and nutrient cycling [1]. Accordingly, most sequenced bacterial isolates contain prophage genomes, but general knowledge of prophage induction frequencies and induction signals is still lacking. Known prophage induction signals are generally related to host DNA damage, activation of the SOS response, and a poor metabolic state of the host cell [2–4]. In addition, prophage induction can occur in a stochastic process known as spontaneous prophage induction (SPI). For most prophages it is, however, unknown whether SPI is truly stochastic, or if additional environmental signals, such as cell-density-dependent signal molecules, could modulate the probability of prophage induction [4, 5].

Many bacterial species can regulate gene expression according to the cell density of the population. They do so in a process known as quorum sensing (QS) by producing, releasing, and subsequently detecting, extracellular signaling molecules called autoinducers [6, 7]. QS is widely used

These authors contributed equally: Demeng Tan, Mads Frederik Hansen

Supplementary information The online version of this article (https://doi.org/10.1038/s41396-020-0641-3) contains supplementary material, which is available to authorized users.

✉ Mathias Middelboe
mmiddelboe@bio.ku.dk

✉ Sine Lo Svenningsen
sls@bio.ku.dk

[1] Shanghai Public Health Clinical Center, Fudan University, Shanghai, China

[2] Dalian SEM Bio-Engineering Technology Co. Ltd, Dalian, China

[3] Department of Biology, University of Copenhagen, Copenhagen, Denmark

[4] Present address: Max Planck Institute for Terrestrial Microbiology, Marburg, Germany

by bacteria to co-ordinate complex behaviors such as virulence [8–11] and biofilm formation [12–15]. In addition, several recent examples have implied a role for QS that goes beyond coordinating the bacterial population, namely QS-regulation of phage-host interactions [16–21]. For example, a number of proteins that serve as phage receptors are known to be QS regulated, meaning that the susceptibility of bacteria to attack by the affected phages is subject to QS control [16–18, 21]. Notably, *Vibrio* phage VP882 was recently shown to encode a QS receptor, which can control prophage induction in response to an autoinducer produced by the host [22]. Although conditions that activate expression of the QS receptor have not yet been identified, this study demonstrated the ability of bacterial QS to affect prophage induction [22]. In line with this, *E. coli* ATCC 15144 was recently found to harbor a pseudolysogenic prophage, in which a regulatory protein was derepressed by the presence of the interspecies autoinducer AI-2. As a result hereof, AI-2 activated the expression of lytic genes, facilitating bacterial lysis [23]. Also, the phage-encoded QS-like arbitrium system, originally discovered in SpBeta *Bacillus* phages [24] has been shown to regulate the lysis-lysogeny switch of some phages [24–26]. In light of the importance that host cell availability must have for phage fitness, and conversely the detrimental effects that the spread of a phage infection can have on a dense bacterial population, it is perhaps not surprising that both host antiphage mechanisms and phage developmental switches have evolved to factor in cell density. However, the extent to which QS regulates phage-host interactions is still largely unknown, and its potential implications for phage-host dynamics in different environments has not been explored. For example, a recent cross-system analysis showed that the virus-to-microbe ratio, VMR, ranged from 3 to 160, suggesting large differences in the role of viral infections across the studied environments [27]. Overall, the relationship between phage and microbial abundances across large temporal and spatial scales has demonstrated nonlinearity, with decreasing VMR at increasing cell densities [27, 28]. In the so-called Piggyback-the-Winner model, Knowles et al. [28] proposed increasing importance of lysogeny at increasing microbial densities as the key driver of this nonlinear relationship. This hypothesis has since been subject to debate [29–33], and there is currently no consensus on the role of the lysis-lysogeny switch of temperate phages explaining the observed decrease in VMR with increased bacterial cell density. If the examples highlighted above are representative of many phage-host interactions, then the study of QS-controlled changes in the lysis-lysogeny shifts is likely to provide new insight into the underlying mechanisms for the decrease in VMR with increasing cell density.

We have used the marine pathogenic Gram-negative bacterium *Vibrio anguillarum* as a model for studying the role of QS in phage-host interactions in marine bacteria. *V. anguillarum* represents a major challenge for the aquaculture industry worldwide, leading to high mortality in numerous shellfish and fish species, and significant economic losses [34, 35]. Genome sequencing of numerous *V. anguillarum* isolates has uncovered the genetic diversity and spatiotemporal dynamics of the pathogen, and has shown the presence of inducible or cryptic prophages in all sequenced isolates [36–40]. *V. anguillarum* employs three autoinducer synthase-receptor pairs [41], and another two are predicted based on the presence of genes homologous to known synthase-receptor pairs in other *Vibrios* [41–43] (See Supplementary Fig. 1). The best studied QS-regulator of *V. anguillarum* is the transcription factor VanT, which is activated at high-cell density in response to extracellular autoinducer molecules [7]. At low autoinducer concentrations (i.e., low-cell density), the response regulator VanO is activated by phosphorylation via a phosphorelay originating from the autoinducer-free receptors. Phosphorylated VanO represses the expression of VanT by activating a set of quorum regulatory RNAs (Qrr) that pair with the *vanT* mRNA. At high-cell densities, autoinducer concentrations rise and the autoinducers bind their cognate membrane-bound receptors. As a result, VanO is dephosphorylated, Qrr transcription ceases, and VanT expression is derepressed, allowing regulation of genes that are under QS control.

Here, we investigate the effect of QS on the interations between *V. anguillarum* strain 90-11-287 and its H20-like prophage p41 [44]. ϕH20-like phage particles have been isolated across Europe and Chile from aquaculture and environmental sites, and have shown their potential for lysogenic conversion and interactions with *V. anguillarum* across large spatial scales [39]. We show that QS represses the induction of the H20-like prophage, resulting in 27-fold more free ϕVa-90-11-287_p41 phage particles in dense lysogenic cultures of a *V. anguillarum* mutant locked in the low-cell-density QS state than in the lysogenic mutant locked in the high-cell-density state. To the best of our knowledge, this report is the first example of QS-mediated repression of prophage induction in any bacterium. Our finding provides indirect experimental support for the Piggyback-the-Winner hypothesis, suggesting that *V. anguillarum* has evolved to actively maintain lysogeny at high-cell densities. Furthermore, we show that the low-cell-density QS state is associated with enhanced biofilm formation and that the H20-like prophage promotes aggregation in this state. In contrast, the expression of proteolytic enzymes is induced in the high-cell-density QS state, perhaps indicating a QS-activated dispersal mechanism as well as antiphage proteolytic defense. The formation of biofilm

is important for *V. anguillarum* colonization and infection of fish [45] and the relationship between QS and biofilm formation has been suggested to be essential for orchestrating infectivity, colonization, and pathogenesis of other *Vibrio* species [46], highlighting the potential relevance of this study for understanding the underlying mechanisms of vibriosis outbreaks caused by *V. anguillarum*.

Materials and methods

Strain, medium and growth conditions

Bacterial strains and plasmids utilized in this study are listed in Supplementary Table 1. *V. anguillarum* was routinely grown in Lysogeny broth Miller (LM) (1% tryptone, 0.5% yeast extract, and 1% NaCl) with aeration or on LM plates at 30 °C. Antibiotics were added when appropriate at the following concentrations: 100 μg·ml^{-1} ampicillin, 25 μg·ml^{-1} chloramphenicol (for *E. coli*), and 5 μg·ml^{-1} chloramphenicol (for *V. anguillarum*).

DNA manipulation

To construct chromosomal deletions in *V. anguillarum* 90-11-287, the flanking regions of the target gene were cloned into pDM4 [47]. The plasmid was transferred into *V. anguillarum* 90-11-287 via conjugation with *E. coli* S17-1 λ-pir harboring the resulting plasmid. Transconjugants were selected on Thiosulfate Citrate bile salts sucrose (TCBS, Becton Dickinson, NJ, USA) or TCI (0.5% sodium thiosulphate, 3.9% Columbia blood agar base, 4.6% potassium iodide, and 0.5% sodium chloride) plates containing 5 μg·ml^{-1} chloramphenicol, followed by selection for plasmid loss on LB plates containing 5% sucrose. The use of TCI agar instead of TCBS consistently resulted in a higher fraction of transconjugants carrying the desired mutation, presumably because the selection for sucrose-tolerant mutants yields false positives when transconjugants are grown on TCBS and therefore preselected for some degree of sucrose tolerance. For Δ*vanT* and Δ*vanO* mutant construction, the pDM4vanT and pDM4vanO plasmids were constructed as described previously [17, 47], using the same primers as in Tan et al. [17]. The ΔH20 deletion plasmid, pDM4H20, was constructed using the primers listed in Supplementary Table 2. Due to ambiguities in the genome sequence, we could not construct a precise deletion of the prophage. Subsequent genome sequencing revealed that the mutant, ΔH20, contains the first 62 bp and the last 7250 bp of the prophage genome, meaning that 45929 bp of the p41 genome were deleted. Further analysis confirmed that the ΔH20 mutant does not produce infective p41 phage particles.

Quantification of *vanT* mRNA levels and AHL production

Overnight cultures of *V. anguillarum* 90-11-287 were back-diluted 1:1000 in LM broth and grown at 30 °C. Aliquots were harvested every hour (starting at 2 h incubation) for determination of acyl-homoserine-lactone autoinducers (AHL) autoinducer levels and for extraction of RNA for *vanT* mRNA quantification. AHL biosynthesis was assayed using an *E. coli* MC4100 pAHL-*gfp* reporter strain with a plasmid-borne fusion of the AHL-induced *V. fischeri lux* operon to *gfp* [48] as in [17].

Aliquots for mRNA quantification by qRT-PCR were immediately mixed with 0.2 volumes stop solution (5% phenol in ethanol) on ice. RNA was extracted using Trizol (Thermo Fisher Scientific, MA, USA) and chloroform, reverse transcribed, and the levels of *vanT* mRNA relative to *recA* mRNA (reference RNA) were determined by qRT-PCR exactly as described previously for *ompK* mRNA [17] using the primers listed in Supplementary Table 2.

Measurement of free ϕH20-like phage particles in lysogenic cultures

Overnight cultures of *V. anguillarum* 90-11-287 wildtype, Δ*vanT*, and Δ*vanO* strains were diluted 1:5000 in LM medium supplemented with 10 mM $MgSO_4$ and 5 mM $CaCl_2$, and grown at 30 °C with aeration. Culture aliqouts were harvested and pelleted by centrifugation for 2.5 min at 16,000 × *g*. The concentration of infective ϕH20-like phage particles in the supernatants were quantified by plaque assay on the ϕH20-sensitive *V. anguillarum* strain BA35 [49]. Bacterial culture densities were measured by monitoring OD_{600} and plating for colony forming units (CFU). A conversion factor of $7.7*10^8 \pm 3.3*10^8$ CFU/ml/OD_{600} was determined as shown in Supplementary Fig. 2. For Fig. 1a, time point $t = 0$ h only, we estimated the correct OD_{600}–value based on the exponential growth curve that best fit the timespan $t = 1$ h to $t = 4$ h (Fig. 1b), because the OD_{600}–measurements at $t = 0$ h were too low to be accurately measured in our spectrophotometer.

Effect of cell-free spent medium on ϕH20-like phage accumulation

Overnight cultures of *V. anguillarum* BA35 were diluted 1:1000 in LM broth, and grown at 30 °C with aeration until OD_{600} reached 0.8. Cell-free spent medium was prepared by centrifugation of an aliqout of the BA35 culture at 12,000 × *g* for 10 min at 4 °C followed by filtration of the supernatant (0.45 μm). Overnight cultures of *V. anguillarum* 90-11-287 wildtype, Δ*vanT*, and Δ*vanO* strains were diluted 1:1000 in the cell-free spent medium, and grown at 30 °C with

aeration. Samples were collected every hour for 8 hours for measurements of bacterial cell density (OD_{600}) and phage particle enumeration by plaque assay.

Phage H20 adsorption rate measurements

Overnight cultures of *V. anguillarum* 90-11-287 ΔH20, Δ*vanT* ΔH20, and Δ*vanO* ΔH20 strains were diluted to OD_{600} ~0.005 in LM medium and grown at 30 °C with aeration until $OD_{600} = 0.5–0.7$. Phages were added at a ratio of 0.0005 PFU/CFU. Aliquots were retrieved at 2, 8, 16, 32, and 64 min after phage addition, centrifuged at 12,000 x *g* for 1 min, and phage particles in the supernatant were enumerated by plaque assay. Adsorption rates were calculated based on the average of three independent experiments, as the slope of the function $y = (\ln(P_0)\text{-}\ln(P))/B_0$, where P_0 and B_0 are the numbers of phages and bacteria added at $t = 0$, respectively.

Quantification of biofilm formation

A Calgary Biofilm Device was used to quantify biofilm formation [50]. Overnight cultures of *V. anguillarum* 90-11-287 wildtype, ΔH20, Δ*vanT*, Δ*vanT* ΔH20, Δ*vanO*, and Δ*vanO* ΔH20 strains were diluted 1:100 in marine broth (MB) (0.5% tryptone, 0.1% yeast extract and 2% sea salts (Sigma-aldrich)) and grown at 30 °C with aeration for 2 h. The cultures were adjusted to $OD_{600} = 0.15$ and transferred into 96-well plates with a Nunc-TSP peg lid system and incubated under static conditions for 48 h at 30 °C for biofilm formation and quantification as described previously [51].

Quantification of aggregation by confocal laser scanning microscopy

Exponential cultures of *V. anguillarum* 90-11-287 wildtype, ΔH20, Δ*vanT*, Δ*vanT* ΔH20, Δ*vanO*, and Δ*vanO* ΔH20 strains were adjusted to $OD_{600} = 0.15$ in MB and transferred to a black 96-well microtiter plate (with transparent bottom (ibidi, Germany)) and incubated for 48 h at 30 °C. Subsequently, planktonic cells were removed by pipetting before staining the biofilm using the FilmTracer™ LIVE/DEAD® Biofilm Viability Kit (Invitrogen, CA, USA). Living cells stained with SYTO9 and compromised cells stained with propidium iodide were excited with lasers at 488 nm and 561 nm, respectively. Z-stack images of an 159.73 × 159.73 µm area were acquired from three different positions in each well with a CLSM instrument (Zeiss LSM800, Carl Zeiss Inc., Germany) equipped with a 40× air objective. The three images acquired from each well were used for averaging and the experiment was replicated four times. Preparation and loading of images were performed as described previously [52] in RStudio [53] using the biovolume elasticity method for automatic thresholding [54] and a previously described function for detection and quantification of aggregates [55].

Quantification of proteolytic acticity

5 µl of overnight cultures of *V. anguillarum* 90-11-287 wildtype, ΔH20, Δ*vanT*, Δ*vanT* ΔH20, Δ*vanO,* and Δ*vanO* ΔH20 mutants were inoculated on solidified MB agar (1.5%) supplemented with 2% skim milk (Sigma-Aldrich, MO, USA) as an indicator for extracellular proteolytic activity. The diameter of each clearing zone was measured after 36 h of incubation at 30 °C.

Overnight cultures of *V. anguillarum* 90-11-287 ΔH20, Δ*vanT* ΔH20, and Δ*vanO* ΔH20 mutants were diluted 1:100 in LM broth and incubated at 30 °C with shaking. At $OD_{600} = 0.1$, 0.7, and following 24 h of incubation (OD_{600}~2.1) aliquots of the cultures were used to quantify proteolytic activity. Bacteria were removed by centrifugation at 6000 × *g* for 10 min at 4 °C and the supernatants were filtered through 0.22 µm-pore size filters before 10 µl were spotted onto MB agar supplemented with 2% skim milk. The diameter of each clearing zone was measured after 36 h of incubation at 30 °C.

Effects of cell-free spent medium on phage particle halflife

Overnight cultures of *V. anguillarum* 90-11-287 ΔH20, Δ*vanT* ΔH20, and Δ*vanO* ΔH20 strains were diluted 1:100 in LM broth and incubated at 30 °C with shaking for 24 h. Subsequently, bacteria were removed by centrifugation at 6000 × *g* for 10 min at 4 °C and filtration through 0.22 µm-pore size filters. Phage stocks of free ϕH20 and KVP40 were adjusted to ~10^6 PFU/ml and mixed with cell-free spent medium in a 1:2 ratio. Samples were incubated at 30 °C for 48 h with aeration before the concentration of infective phages was quantified by plaque assay on susceptible strains (PF430-3 Δ*vanT* for KVP40 and BA35 for ϕH20). The reduction of infective phage concentration in cell-free spent medium was determined by comparing the phage titer with the respective titer after incubation in LM broth.

Results

Accumulation of ϕH20 particles is highly dependent on the status of the host QS system

V. anguillarum isolate 90-11-287 carries the H20-like prophage p41 [38], and produces ϕH20-like ϕVa-90-11-287_p41

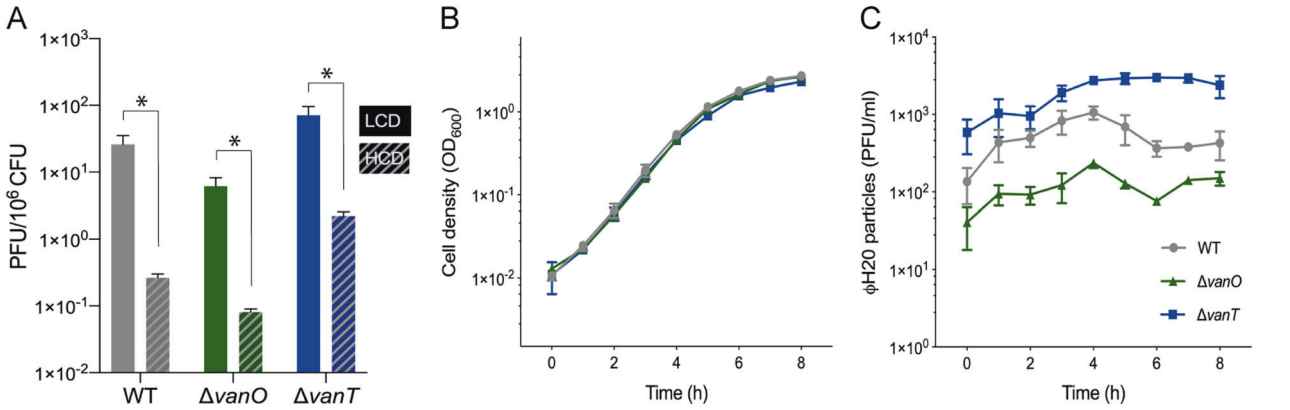

Fig. 1 Free ΦH20 particles accumulate in cultures of lysogens in a QS-dependent manner. (**a**) The concentration of plaque forming units (PFU ml^{-1}) in cell-free spent supernatants from cultures of *V. anguillarum* isolate 90-11-287 wildtype (WT), and QS mutant strains (Δ*vanT* and Δ*vanO*) is shown relative to the concentration of bacterial colony forming units (CFU ml^{-1}) in the cultures at the time of phage harvest. Solid bars represent the average of all the low-cell-density data points from Fig. 1C (LCD: $OD_{600} < 0.05$) and hatched bars represent the average of all the high-cell-density data points from Fig. 1C ($OD_{600} > 1.0$). An asterisk indicates a significant difference between LCD and HCD conditions (Welch's *t* test, $\alpha = 0.05$) and error bars represent the standard error of the mean *($N = 6–8$ for LCD and $N = 10–11$ for HCD)* (**b**) Optical densities (OD_{600}) of cultures of wildtype (WT) and QS mutant strains (Δ*vanT* and Δ*vanO*) were measured at 1 h intervals during growth from low to high cell density. (**c**) The corresponding concentrations of phage particles in the cultures (PFU ml^{-1}) were measured by plaque assay. For (**b**) and (**c**), symbols represent the averages of triplicate independent experiments. Time = 0 h indicates the time of the first measurement.

phage particles at a low rate that is ascribed to SPI events. As shown in Fig. 1a (WT, gray bars), low-cell-density cultures of strain 90-11-287 contain on the order of 20-30 ϕH20-like extracellular phage particles per million lysogens, while the phage-to-cell ratio is reduced by 100-fold when the cultures have grown to high cell density.

To investigate whether cell-density-dependent signals affected prophage induction, we first confirmed key features of the QS system in *V. anguillarum* 90-11-287. Previous research [41, 59] suggested that the VanT-dependent QS circuit of *V. anguillarum* might not function in a manner fully equivalent to the canonical pathway, which has been described in detail in *V. cholerae* and *V. harveyi* [58]. In particular, *vanT* mRNA was only moderately reduced at low cell density compared with high cell density in *V. anguillarum* strain NB10 [59], while *vanT* expression would be repressed at low cell densities in the canonical circuit (see Supplementary Fig. 1 for details). In order to determine whether *vanT* mRNA levels increased in a cell-density-dependent manner in *V. anguillarum* 90-11-287, we measured *vanT* mRNA levels and extracellular levels of AHL during growth in batch culture. As shown in Supplementary Fig. 3, AHL levels rose with increasing optical density of the culture, and the *vanT* mRNA levels per cell increased more than 30-fold during growth from low to high cell density. Thus, with respect to regulation of the *vanT* mRNA levels, the QS circuit of *V. anguillarum* strain 90-11-287 appears to function analogously to the canonical circuit, and different from *V. anguillarum* strain NB10.

To directly examine the effects of QS on the interaction between *V. anguillarum* 90-11-287 and the H20-like prophage, two otherwise isogenic QS mutants were constructed. A Δ*vanO* mutant is expected to express high levels of VanT independent of population density and is therefore locked in a high-cell-density QS mode. By contrast, a Δ*vanT* mutant has lost the ability to activate QS-associated functions and is therefore locked in a low-cell-density mode. By monitoring the concentrations of cells and infective phage particles during the growth of lysogenic batch cultures, we found that the bacterial growth rate exceeded the rate at which phages accumulated in all three strains, resulting in significantly lower phage-per-cell ratios at high cell densities than at low cell densities (Fig. 1a). However, deletion of the QS regulators had strong effects on the dynamics of phage particle accumulation in the cultures, and on the resulting phage-to-cell ratio at high cell densities. Although the three strains grew at similar rates (Fig. 1b), the wildtype cultures initially showed an increase in the concentration of free ϕH20-like phages during growth, which was followed by a drop in the phage concentration as the OD approached 1, and ended at ~400 PFU ml^{-1} at the highest cell densities (Fig. 1c, gray circles). By contrast, phage particles accumulated somewhat throughout growth in the QS-deficient Δ*vanT* mutant, stabilizing at ~2900 PFU ml^{-1} (Fig. 1c, blue squares). Finally, cultures of the Δ*vanO* mutant showed a lower phage concentration than the wildtype at all cell densities (Fig. 1c, green triangles). Thus, the VanT QS circuit has a strong effect on the interactions of the H20-like prophage p41 with its host.

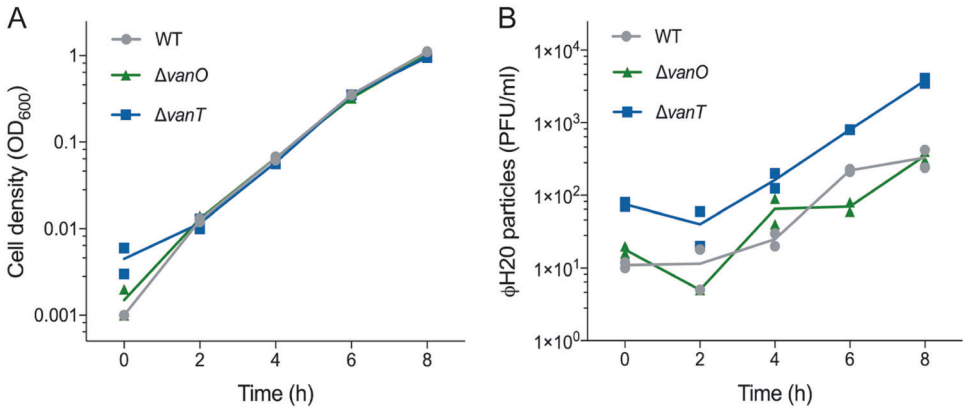

Fig. 2 An extracellular molecule(s) controls accumulation of ΦH20-like phage particles. (**a**) Optical densities (OD_{600}) of cultures of *V. anguillarum* wildtype, Δ*vanT*, and Δ*vanO* strains were measured at 2 h intervals over an 8 h period of incubation in the presence of cell-free spent supernatant obtained from a culture of wildtype *V. anguillarum* BA35 grown to mid-log phase. The depicted variation in cell density measured at the initial timepoint is largely due to the technical limitations of the spectrophotometer, as the values are at or below the detection limit of the instrument. (**b**) The corresponding abundances of phage particles per milliliter (PFU ml^{-1}) were quantified by plaque assay. Lines represent the averages of duplicate measurements represented as symbols.

An extracellular factor present in cell-free supernanants regulates ϕH20-like phage accumulation

To test if an extracellular factor, such as a QS autoinducer, was involved in the regulation of ϕH20-like phage accumulation, we examined the effect of adding cell-free spent culture supernatant from high-cell-density cultures of *V. anguillarum* to freshly inoculated cultures of the lysogenic strain 90-11-287. We avoided introducing ϕH20-like particles with the supernatant by using supernatant from *V. anguillarum* strain BA35, which does not carry H20-like prophages. During exposure to BA35 supernatant, the 90-11-287 wildtype cultures accumulated phage particles at the same rate as cultures of the *ΔvanO* mutant (Fig. 2a, b), suggesting that with regards to phage accumulation, the addition of cell-free spent supernatant to the wildtype strain is equivalent to locking the bacteria in the high-cell-density state of the *ΔvanO* mutant. Furthermore, the addition of cell-free spent supernatant did not similarly reduce phage accumulation in the Δ*vanT* mutant cultures, which are incapable of responding to autoinducers through the canonical VanT pathway. These results support the hypothesis that an extracellular factor(s), likely an autoinducer, controls free phage accumulation via the VanT-dependent QS pathway.

Altered phage adsorption rates cannot explain the QS-effect on phage particle accumulation

The concentration of free phage particles present in the culture medium is not only a function of the rate at which phage particles are released by prophage induction, but also a function of the rate of phage loss, which depends on the rate at which the released phage particles adsorb to and superinfect the lysogenic cells in the culture, and the half-life of the phage particles in the extracellular medium. If any of these factors differ between the QS mutants, it would be predicted to lead to a difference in the number of free phage particles observed in the cultures of lysogens. For example, prophage induction of coliphage λ^{i434} was initially reported to be induced by QS because phage particles produced by a culture of *Escherichia coli* lysogens accumulated extracellularly to a greater extent in the presence of AHL than in its absence [5]. However, further studies revealed that prophage induction was not affected by AHL. Rather, the presence of AHL lead to down-regulation of the λ receptor protein, resulting in a reduced rate of superinfection by released phages, and thus causing increased extracellular accumulation of phage particles in the presence of AHL [16].

The means by which ϕH20-like phages infect *V. anguillarum* has not yet been identified, so we could not test directly whether the phage receptor was QS regulated. Instead, we quantified the rate of adsorption of the ϕH20-like phage to cells of wildtype, Δ*vanO* and Δ*vanT* cultures to investigate whether the increase in phage particles seen in the Δ*vanT* mutant cultures could be explained by a relative decrease in the rate of phage adsorption to Δ*vanT* cells. To avoid interference by phage particles released from the lysogenic cells, we first deleted the prophage genome from the strains using homologous recombination (denoted as ΔH20, see "Materials and Methods"). ϕH20-like phages did not adsorb slower to the Δ*vanT* ΔH20 strain than to the two other strains (Fig. 3), demonstrating that the increased accumulation of free phage particles in the Δ*vanT* mutant (Fig. 1c) was not due to a reduced rate of phage readsorption in this strain. We consistently observed a trend that

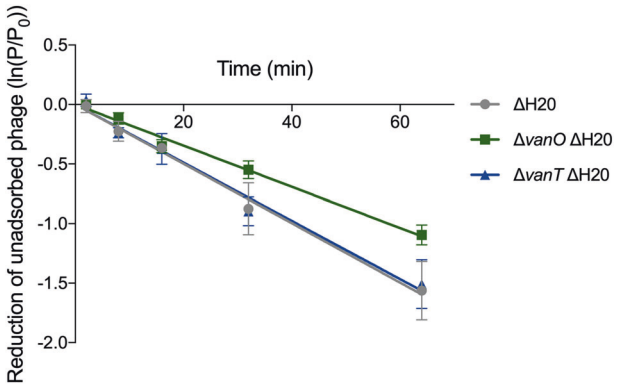

Fig. 3 Similar adsorption rates of ϕH20-like phages to ΔH20, *ΔvanT* ΔH20, and *ΔvanO* ΔH20 mutant cells. Exponentially growing cultures of the indicated strains at $OD_{600} = 0.6–0.9$ were mixed with a lysate of ϕH20-like phage p41. At the indicated time points, unadsorbed phage enumerated by plaque assay. Shown is the average of three independent experiments. Error bars indicate the standard error of the mean ($N = 3$). Adsorption rate constants ($4.0 \times 10^{-11} \pm 0.8 \times 10^{-11}$ PFU × ml per minute per bacterium for the ΔH20 mutant that is wildtype with regards to the QS system, $4.2 \times 10^{-11} \pm 1.7 \times 10^{-11}$ for the *ΔvanT* ΔH20 mutant, and $2.9 \times 10^{-11} \pm 0.5 \times 10^{-11}$ for the *ΔvanO* ΔH20 mutant) are not significantly different (*linear regression analysis with Tukey adjustment*, $P = 0.16$, $\alpha = 0.05$).

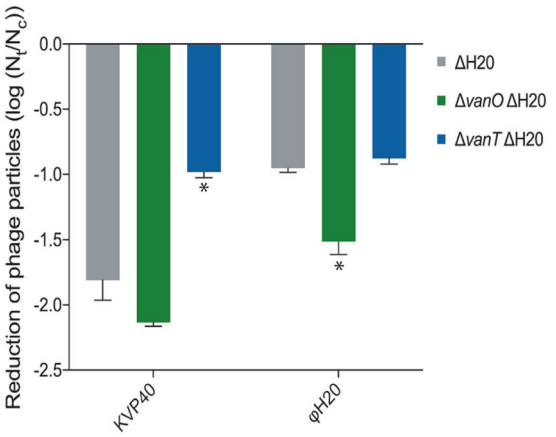

Fig. 4 Extracellular proteolytic activity reduces the number of infective phage particles. Concentration of KVP40 (*Myoviridae*) and ϕH20 (*Siphoviridae*) was reduced post 48 h of incubation in cell-free spent supernatant (N_t) compared with incubation in growth medium (control, N_c). An asterisk indicates a significant reduction of infective phages compared with cell-free spent supernatants from the ΔH20 cultures (*ANOVA and Sidak's multiple comparison test*, $\alpha = 0.05$). Error bars represent standard error of the mean ($N = 3$).

ϕH20-like phages adsorbed more slowly to the Δ*vanO* ΔH20 mutant cells than to the ΔH20 and Δ*vanT* ΔH20 mutants, which could indicate QS-regulation of the unidentified phage receptor, but the difference was not statistically significant.

QS regulates *V. anguillarum* proteolytic activity and affects phage particle stability

An alternative explanation for the relatively high abundance of free phage particles in cultures of the Δ*vanT* mutant is that the free ϕH20-like phage particles may be more stable in the medium of Δ*vanT* mutant cultures than in the medium of wildtype and Δ*vanO* mutant cultures. Quantification of the proteolysis of skim milk proteins revealed that proteolytic activity was indeed reduced in the Δ*vanT* mutant compared with the wildtype, while the Δ*vanO* mutant showed slightly higher proteolytic activity (Supplementary Fig. 4A). No differences were observed when comparing otherwise isogenic strains with and without the prophage, indicating that the presence of the H20-like prophage did not affect proteolytic activity in any of the strains (Supplementary Fig. 4A). Spotting cell-free spent supernatants collected from the prophage-free strains at low, intermediate and high bacterial densities on skim-milk plates demonstrated that the diameter of the clearing zone increased proportionally with the bacterial density for the Δ*vanO* ΔH20 mutant, as would be expected if the cells are constitutively producing extracellular proteases (Supplementary Fig. 4B, green triangles). In contrast, no clearing zones were observed when spotting the cell-free supernatants collected from the Δ*vanT* ΔH20 mutant (Supplementary Fig. 4B, blue squares). Finally, the ΔH20 mutant which has a wildtype QS-circuit showed limited protease activity at the low and intermediate cell densities, but at high-cell densities, proteolytic activity was similar to that of the Δ*vanO* ΔH20 mutant (Supplementary Fig. 4B, gray circles). Thus, proteolytic activity of strain 90-11-287 is under strong positive regulation by the VanT QS system.

To test whether these differences influenced the stability of phage particles, we incubated phage ϕH20 (*Siphoviridae*) and phage KVP40 (*Myoviridae*) particles in cell-free spent medium from the ΔH20 strain set and enumerated remaining phage particles relative to the phage titer of control samples incubated in growth medium (Fig. 4).

In all cases, phage titers were lower after incubation in cell-free spent medium relative to the control. Furthermore, the QS-state of the cultures from which the cell-free spent medium originated affected the lifetime of both KVP40 and ϕH20 particles. Specifically, the stability of KVP40 particles was significantly higher in cell-free spent supernatant from the Δ*vanT* mutant relative to the wildtype and the Δ*vanO* mutant, and the stability of ϕH20 particles was significantly higher in cell-free spent medium from the Δ*vanT* mutant and the wildtype relative to the Δ*vanO* mutant (Fig. 4). These data support that QS-controlled protease expression could function as an antiphage strategy in *V. anguillarum* strain 90-11-287. However, the

magnitude of the difference in number of remaining ϕH20 infective particles after 48 h incubation with medium from the two locked QS mutants (Δ*vanO* and Δ*vanT*) was only 3.8-fold. It is therefore unlikely that the observed 27-fold difference in phage particles accumulating in lysogenic cultures (Fig. 1a) is due to the difference in phage particle lifetime in the growth medium of the Δ*vanO* and Δ*vanT* mutant cultures. In support of this argument, the difference in phage particle accumulation reported in Fig. 1 is notable also in the beginning of the experiment where the cultures are still at low cell density (Fig. 1c) and have not yet accumulated appreciable concentrations of extracellular proteases (Supplementary Fig. 4B).

Since the accumulation of phage particles in lysogenic cultures of the Δ*vanT* mutant cannot be explained by reduced adsorption rates (Fig. 3) or increased phage particle lifetime (Fig. 4), we conclude that VanT-dependent QS represses the induction of the H20-like prophage.

Biofilm formation is repressed by QS and enhanced by the H20-like prophage

To begin to identify any effects that the H20-like prophage may have on the properties of its host, we first tested how QS affected biofilm formation in strain 90-11-287 by quantifying biofilm formation of the wildtype and QS mutants using crystal violet staining. Strain 90-11-287 was in general a poor biofilm former under the tested conditions, but the Δ*vanT* mutant formed substantially more biofilm than both the wildtype and the Δ*vanO* mutant (Fig. 5a, solid bars). Therefore, we consider biofilm formation a QS-repressed trait in strain 90-11-287. Next, we used our ΔH20 strain set to investigate the potential role of the H20-like prophage on biofilm formation. Interestingly, deletion of the H20 prophage in the Δ*vanT* mutant reduced biofilm formation (Fig. 5, Δ*vanT* ΔH20 double mutant). Confocal laser scanning microscopy of mature biofilms supported that the H20-like prophage affected *V. anguillarum* aggregation at low cell density (Supplementary Fig. 5). In particular, the prophage was shown to be important for the formation of relatively large aggregates (>28 μm^3), the occurrence of which was significantly reduced in the Δ*vanT* ΔH20 double mutant compared with the Δ*vanT* mutant containing the prophage (Fig. 5b).

Discussion

Here, we show that QS represses prophage induction and increases extracellular proteolytic digestion of phage particles in *V. anguillarum*, emphasizing that central aspects of phage-host interactions, such as the lysis-lysogeny switch and antiphage defense mechanisms, depend on the density of the host population. In a broader context, these results provide new insight into the drivers of the lysis-lysogeny switch in marine microbial communities, and point to an increasing prevalence of lysogeny at increasing cell densities. Our work thus contributes important input to the current discussion on the mechanisms underlying the recent observations of decreasing VMR with increasing cell densities in the marine environment [27–30, 56]. By demonstrating that repression of prophage induction rates occur in response to activation of the host QS pathway in *V. anguillarum*, our findings support the proposed Piggyback-the-Winner model, which contends that lytic dynamics are suppressed at high cell

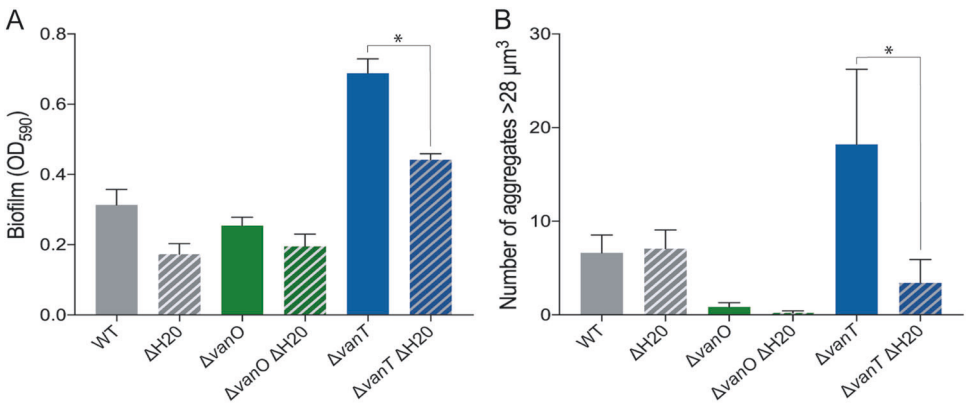

Fig. 5 Biofilm formation and aggregation of *V. anguillarum* 90-11-287 is enhanced at low-cell density and affected by the H20-like prophage. (**a**) Quantification of biofilm formation after 48 h of incubation. (**b**) Aggregates with a biovolume larger than 28 μm^3 based on CLSM z-stack images in an area of 159.73 × 159.73 μm. An asterisk indicates a significant difference between the prophage-harboring and prophage-free mutants (*ANOVA and Tukey's multiple comparison test,* $\alpha = 0.05$) and error bars represent standard error of the mean ($N = 3$ *for crystal violet assays and* $N = 4$ *for CLSM quantification).*

densities [28], and our results suggest that QS could play a key role as a regulatory link between host cell density and prophage induction rates.

QS control of prophage induction

Intuitively, increased prophage induction at high-cell-density conditions would confer a selective advantage on the phage if it increases the chance that phage progeny rapidly meets new hosts [57, 60]. However, as pointed out recently [61] eavesdropping on the host's QS system will not on its own provide the prophage with that information, because QS does not reveal whether surrounding autoinducer-producing bacteria are susceptible, immune or resistant to the phage. At first glance, the observed stabilization of the lysogenic state at high cell densities stands in contrast to other studies, which have found that lysogeny prevailed when ecosystem productivity [62], levels of glucose [23] or bacterial production [60] was low, generally representing low-cell-density conditions. Although vibrios are highly abundant in aquatic environments, the cell densities used in these experiments (ranging from ~10^6 to 10^9 bacteria ml^{-1}) are most likely to be found in bacterial communities associated with eukaryotic marine organisms [63], or in aquaculture facilities, where specific pathogenic vibrios are often observed in densities of up to 10^8 ml^{-1} [64]. We emphasize that QS-regulation of H20-like prophage induction is not an all-or-none phenomenon. The probability for a lysogen to produce phage particles was estimated to be on the order of 10^{-6}–10^{-7} per generation in our experiments, based on the phage-to-cell ratio at low cell densities (when superinfection would be minimal) and a burst size of 50−100. Free phage accumulation differed 27-fold between the two QS-locked mutants (Fig. 1a), demonstrating that QS modulates the rate of prophage induction while leaving plenty of room for additional cues, such as host metabolic state, to also affect prophage induction rates. Similarly, in the case of prophage VP882, high prophage induction rates were only observed when the phage-encoded QS receptor was artificially induced, and therefore the magnitude of the QS effect on VP882 induction is not yet known [22]. Thus, while adding to our understanding of the factors controlling the lysis-lysogeny switch in an important group of marine bacteria, our study also underlines the need for further studies to resolve the regulation of lysogeny in different bacteria and across gradients in cell density and productivity.

Prophage retention as a host strategy

A prophage element represents a hereditary biosynthetic burden, but the continued presence of the phage genome in the host also provides an opportunity for the evolution of functions that benefit the host or provides mutual benefits for the phage and the host [4, 65–68]. *Vibrio* prophages are known to encode important virulence genes [40], which may promote infection of animal hosts at high cell densities. Active retention of prophages at high cell densities may therefore play a key role in *V. anguillarum* pathogenicity, and may indeed be a selective advantage from the host perspective. Another phenotypic trait that can be strongly affected by phages is the production of biofilm [66]. Increased biofilm formation can be facilitated by induction of prophages that strengthen the biofilm matrix by releasing various components such as eDNA [69–71]. We observed that the H20-like prophage increased the host population's biofilm formation, and in particular the formation of large aggregates in the low-cell-density state, thus supporting the surface-associated growth that is required for colonization of fish tissue [45]. We speculate that increased induction of the H20-like prophage in the low-cell-density QS state, where *V. anguillarum* 90-11-287 produces biofilm, could benefit a lysogenic bacterial population during the early stages of animal infection, while retention of the prophage in the high-cell-density QS state could be advantageous during later stages of infection. Thus, rather than explaining the increased lysogeny at high cell density solely as a strategy for the phages to piggyback their hosts, we suggest it also as a host strategy evolved to take control of the lysis-lysogeny switch to promote its own fitness, likely during animal infection. Our results thus support previous suggestions that the interaction between *V. anguillarum* and ϕH20 provides a selective advantage for both the phage and the host, and likely contributes to the successful dispersal of ϕH20-like phages in *V. anguillarum*, as indicated by the efficient spreading and high occurrence (>60% of all sequenced genomes) of ϕH20-like phages among *V. anguillarum* isolates, covering large geographical distances and more than 25 years of isolation [39].

From the viewpoint of an individual bacterium, the risk of a phage attack is generally higher when the surrounding bacterial cell density is high. It is therefore plausible that QS-induced antiphage mechanisms benefit bacteria by specifically upregulating their defense mechanisms under high-risk conditions [16]. We report a reduced lifetime of both ϕH20 and KVP40 phage particles in the high-cell-density state compared with the low-cell-density state, at least partly due to QS control of bacterial proteolytic activity (Fig. 4 and Supplementary Fig. 4). We speculate therefore that QS-controlled repression of prophage induction and stimulation of extracellular proteases at high cell densities are strategies evolved in *V. anguillarum* to prevent superinfection by related phages and retain important prophage-encoded properties, and to inactivate infective phages, respectively.

QS regulation in *V. anguillarum*

QS controls key phenotypic traits of *Vibrio* spp. such as their virulence, biofilm formation, motility, and the production of siderophores and extracellular enzymes [58]. Within *Vibrios* there are examples of both QS-activated and QS-repressed biofilm formation [15, 17, 41, 72]. A *V. anguillarum ΔvanT* mutant of strain NB10 was previously shown to be deficient in biofilm formation [72], indicating that high-cell density promotes biofilm formation. However, the phenotypes of *ΔvanT* and *ΔvanO* mutants in *V. anguillarum* strain PF430-3 suggested the opposite, namely that aggregation was induced in the *ΔvanT* mutant and absent in the *ΔvanO* mutant [17]. Here, we show that QS represses biofilm formation and promotes expression of proteolytic enzymes in *V. anguillarum* strain 90-11-287, as also observed in *V. cholerae* [13, 46]. In combination with the finding that *vanT* mRNA levels were nearly constant in NB10 at different cell densities [59], while we measured a ~31-fold increase over the growth curve (Supplementary Fig. 3), it is clear that large variations in the VanT QS pathway and regulon exist between different strains of *V. anguillarum*.

Our work adds to an increasing body of evidence for an additional important role for QS in *Vibrios*, namely in regulating interactions between the bacteria and the bacteriophages that prey on them [17, 18, 21]. Application of QS inhibitors has been suggested as a potential treatment strategy for bacterial infection [73, 74]. The findings of this study emphasize that in order to fulfill the potential of such a strategy, a comprehensive understanding of phage-host interactions and QS-mediated control of virulence and biofilm formation is required. For ϕH20-lysogenic *V. anguillarum* strains, QS inhibitors could in fact promote biofilm formation and lead to low-level induction of phages that would result in a strengthened biofilm.

Ecological implications

In addition to the adaptive benefits of submitting prophage induction to QS control suggested for the specific bacterial population, a reduced induction of prophages in marine bacteria at high-cell densities potentially also has implications far beyond the effects at the population level. Viral lysis of bacterial cells represents a major contribution of bioavailable organic matter on a global scale, which catalyzes biogeochemical cycling and stimulates bacterial and primary production [75–77]. A reduction in the ratio of lytic to lysogenic infections at increasing cell density would therefore also reduce the role of virus-driven organic matter cycling at these conditions. Consequently, the observed changes in regulation of the lysis-lysogeny switch in response to cell density, and the derived effects on the release of cell lysates, could potentially have large effects on marine elemental cycling, with increasing relative importance of virus-driven biogeochemical cycling in low-cell-density environments. Further studies on the prevalence of quorum-sensing control of prophage induction are therefore essential for a better understanding of the role of viruses in elemental cycling at different environmental conditions.

Acknowledgements This project was supported by the Villum Foundation, Young Investigator Programme (ref. no. 10098) to MB, the Independent Research Fund Denmark (Project # DFF - 7014–00080) to MM, and the Danish National Research Foundation (DNRF120) to SLS. We thank Emilie Søndberg for quantification of infective phage particles, Nanna M.C. Olsen and Jakob Russel for assistance with the quantitative analysis of aggregates, and Prof. Lone Gram, Technical University of Denmark for providing the strain *V. anguillarum* 90-11-287.

Compliance with ethical standards

Conflict of interest The authors declare that they have no conflict of interest.

Publisher's note Springer Nature remains neutral with regard to jurisdictional claims in published maps and institutional affiliations.

References

1. Brussaard CPD, Wilhelm SW, Thingstad F, Weinbauer MG, Bratbak G, Heldal M, et al. Global-scale processes with a nanoscale drive: the role of marine viruses. ISME J. 2008;2:575–8. http://www.ncbi.nlm.nih.gov/pubmed/18385772.
2. Melechen NE, Go G. Induction of lambdoid prophages by amino acid deprivation: differential inducibility; role of recA. Mol Gen Genet. 1980;180:147–55. http://www.ncbi.nlm.nih.gov/pubmed/6449654.
3. Little JW, Mount DW. The SOS regulatory escherichia coli system of review. Cell. 1982;29:11–22.
4. Nanda AM, Thormann K, Frunzke J. Impact of spontaneous prophage induction on the fitness of bacterial populations and host-microbe interactions. J Bacteriol. 2015;197:410–9.
5. Ghosh D, Roy K, Williamson KE, Srinivasiah S, Wommack KE, Radosevich M. Acyl-homoserine lactones can induce virus production in lysogenic bacteria: an alternative paradigm for prophage induction. Appl Environ Microbiol. 2009;75:7142–52.
6. Ng W-L, Bassler BL. Bacterial quorum-sensing network architectures. Annu Rev Genet [Internet]. 2009;43:197–222. http://www.annualreviews.org/doi/10.1146/annurev-genet-102108-134304.
7. Papenfort K, Bassler BL. Quorum sensing signal–response systems in gram-negative bacteria. Nat Rev Microbiol [Internet]. 2016;14:576–88. https://doi.org/10.1038/nrmicro.2016.89.
8. Zhu J, Beaber JW, Moré MI, Fuqua C, Eberhard A, Winans SC. Analogs of the autoinducer 3-oxooctanoyl-homoserine lactone strongly inhibit activity of the TraR protein of Agrobacterium tumefaciens. J Bacteriol. 1998;180:5398–405.
9. Rumbaugh KP, Trivedi U, Watters C, Burton-Chellew MN, Diggle SP, West SA. Kin selection, quorum sensing and virulence in pathogenic bacteria. Proc R Soc B Biol Sci. 2012;279:3584–8.
10. Herzog R, Peschek N, Fröhlich KS, Schumacher K, Papenfort K. Three autoinducer molecules act in concert to control virulence gene expression in Vibrio cholerae. Nucleic Acids Res. 2019;47:3171–83.

11. Grundstad ML, Parlet CP, Kwiecinski JM, Kavanaugh JS, Crosby HA, Cho Y-S. et al. Quorum sensing, virulence, and antibiotic resistance of USA100 methicillin-resistant staphylococcus aureus isolates. mSphere. 2019;4:1–14. https://doi.org/10.1128/mSphere.00553-19.
12. Davies DG, Parsek MR, Pearson JP, Iglewski BH, Costerton JW, Greenberg EP. The involvement of cell-to-cell signals in the development of a bacterial biofilm. Science. 1998;280:295–8. https://doi.org/10.1126/science.280.5361.295.
13. Hammer BK.Bassler BL, Quor sens controls biofilm formation Vibrio cholera. 2003;50:101–14.
14. Nadell CD, Xavier JB, Levin SA, Foster KR. The evolution of quorum sensing in bacterial biofilms. Moran NA, editor. PLoS Biol. 2008;6:e14. https://doi.org/10.1371/journal.pbio.0060014.
15. Passos da Silva D, Schofield M, Parsek M, Tseng B. An update on the sociomicrobiology of quorum sensing in gram-negative biofilm development. Pathogens. 2017;6:51.
16. Høyland-Kroghsbo NM, Mærkedahl RB, Svenningsen S Lo. A quorum-sensing-induced bacteriophage defense mechanism. MBio [Internet]. 2013 Feb 19;4:1–8. http://mbio.asm.org/cgi/doi/10.1128/mBio.00362-12.
17. Tan D, Svenningsen S Lo, Middelboe M. Quorum sensing determines the choice of antiphage defense strategy in Vibrio anguillarum. MBio 2015;6:e00627. https://www.ncbi.nlm.nih.gov/pubmed/26081633.
18. Hoque MM, Naser IBin, Bari SMN, Zhu J, Mekalanos JJ, Faruque SM. Quorum regulated resistance of vibrio cholerae against environmental bacteriophages. Sci Rep. 2016;6:37956. https://doi.org/10.1038/srep37956.
19. Patterson AG, Jackson SA, Taylor C, Evans GB, Salmond GPC, Przybilski R, et al. Quorum sensing controls adaptive immunity through the regulation of multiple CRISPR-Cas systems. Mol Cell. 2016;64:1102–8. https://doi.org/10.1016/j.molcel.2016.11.012.
20. Høyland-Kroghsbo NM, Paczkowski J, Mukherjee S, Broniewski J, Westra E, Bondy-Denomy J, et al. Quorum sensing controls the Pseudomonas aeruginosa CRISPR-Cas adaptive immune system. Proc Natl Acad Sci. 2017;114:131–5. http://www.ncbi.nlm.nih.gov/pubmed/27849583.
21. Castillo D, Rørbo N, Jørgensen J, Lange J, Tan D, Kalatzis PG, et al. Phage defense mechanisms and their genomic and phenotypic implications in the fish pathogen Vibrio anguillarum. FEMS Microbiol Ecol. 2019 Mar 1;95. https://academic.oup.com/femsec/advance-article/doi/10.1093/femsec/fiz004/5281231.
22. Silpe JE, Bassler BL. A host-produced quorum-sensing autoinducer controls a phage lysis-lysogeny decision. Cell. 2018 Dec;1–13. https://linkinghub.elsevier.com/retrieve/pii/S0092867418314582.
23. Laganenka L, Sander T, Lagonenko A, Chen Y, Link H, Sourjik V. Quorum sensing and metabolic state of the host control lysogeny-lysis switch of bacteriophage T1. MBio. 2019;10:3–8. http://www.ncbi.nlm.nih.gov/pubmed/31506310.
24. Erez Z, Steinberger-Levy I, Shamir M, Doron S, Stokar-Avihail A, Peleg Y, et al. Communication between viruses guides lysis–lysogeny decisions. Nature. 2017;541:488–93. http://www.nature.com/doifinder/10.1038/nature21049.
25. Gallego del Sol F, Penadés JR, Marina A. Deciphering the molecular mechanism underpinning phage arbitrium communication systems. Mol Cell. 2019;74:59–72.e3.
26. Stokar-Avihail A, Tal N, Erez Z, Lopatina A, Sorek R. Widespread utilization of peptide communication in phages infecting soil and pathogenic bacteria. Cell Host Microbe. 2019;25:746–55.e5. https://doi.org/10.1016/j.chom.2019.03.017.
27. Wigington CH, Sonderegger D, Brussaard CPD, Buchan A, Finke JF, Fuhrman JA, et al. Re-examination of the relationship between marine virus and microbial cell abundances. Nat Microbiol. 2016;1. https://doi.org/10.1038/nmicrobiol.2015.24.
28. Knowles B, Silveira CB, Bailey BA, Barott K, Cantu VA, Cobián-Güemes AG, et al. Lytic to temperate switching of viral communities. Nature. 2016;531:466–70. http://www.ncbi.nlm.nih.gov/pubmed/26982729.
29. Weitz JS, Beckett SJ, Brum JR, Cael BB, Dushoff J. Lysis, lysogeny and virus–microbe ratios. Nature. 2017;549:E1–3. https://doi.org/10.1038/nature23295.
30. Knowles B, Rohwer F. Knowles & Rohwer reply. Nature. 2017;549:E3–4.
31. Coutinho FH, Silveira CB, Gregoracci GB, Thompson CC, Edwards RA, Brussaard CPD, et al. Marine viruses discovered via metagenomics shed light on viral strategies throughout the oceans. Nat Commun. 2017;8:1–12. https://doi.org/10.1038/ncomms15955.
32. Alrasheed H, Jin R, Weitz JS. Caution in inferring viral strategies from abundance correlations in marine metagenomes. Nat Commun. 2019;10:501. https://doi.org/10.1038/s41467-018-07950-z.
33. Coutinho FH, Silveira CB, Gregoracci GB, Thompson CC, Edwards RA, Brussaard CPD, et al. Reply to: Caution in inferring viral strategies from abundance correlations in marine metagenomes. Nat Commun. 2019;10:502. https://doi.org/10.1038/s41467-018-08286-4.
34. Frans I, Michiels CW, Bossier P, Willems KA, Lievens B, Rediers H. Vibrio anguillarum as a fish pathogen: virulence factors, diagnosis and prevention. J Fish Dis. 2011;34:643–61.
35. Hickey ME, Lee JL. A comprehensive review of Vibrio (Listonella) anguillarum: ecology, pathology and prevention. Rev Aquac. 2017;1893:1–26.
36. Rodkhum C, Hirono I, Stork M, Di Lorenzo M, Crosa JH, Aoki T. Putative virulence-related genes in Vibrio anguillarum identified by random genome sequencing. J Fish Dis. 2006;29:157–66. http://www.ncbi.nlm.nih.gov/pubmed/16533301.
37. Naka H, Crosa JH. Genetic determinants of virulence in the marine fish pathogen vibrio anguillarum. Fish Pathol. 2011;46:1–10. http://www.ncbi.nlm.nih.gov/pubmed/21625345.
38. Castillo D, Alvise PD, Xu R, Zhang F, Middelboe M, Gram L. Comparative genome analyses of Vibrio anguillarum strains reveal a link with pathogenicity traits. mSystems. 2017;2:e00001–17. http://www.ncbi.nlm.nih.gov/pubmed/28293680.
39. Kalatzis P, Rørbo N, Castillo D, Mauritzen JJ, Jørgensen J, Kokkari C, et al. Stumbling across the same phage: Comparative genomics of widespread temperate phages infecting the fish pathogen Vibrio anguillarum. Viruses. 2017;9:1–19.
40. Castillo D, Kauffman K, Hussain F, Kalatzis P, Rørbo N, Polz MF, et al. Widespread distribution of prophage-encoded virulence factors in marine Vibrio communities. Sci Rep. 2018;8:9973. http://www.nature.com/articles/s41598-018-28326-9.
41. Milton DL. Quorum sensing in Vibrios: complexity for diversification. Int J Med Microbiol. 2006;296:61–71.
42. Papenfort K, Förstner KU, Cong J-P, Sharma CM, Bassler BL. Differential RNA-seq of Vibrio cholerae identifies the VqmR small RNA as a regulator of biofilm formation. Proc Natl Acad Sci USA. 2015;112:E766–75. https://www.ncbi.nlm.nih.gov/pubmed/25646441.
43. Ng W-L, Perez LJ, Wei Y, Kraml C, Semmelhack MF, Bassler BL. Signal production and detection specificity in Vibrio CqsA/CqsS quorum-sensing systems. Mol Microbiol. 2011;79:1407–17. http://www.ncbi.nlm.nih.gov/pubmed/21219472.
44. Castillo D, Andersen N, Kalatzis PG, Middelboe M. Large phenotypic and genetic diversity of prophages induced from the fish pathogen Vibrio anguillarum. Viruses. 2019;11:983.
45. Croxatto A, Lauritz J, Chen C, Milton DL. Vibrio anguillarum colonization of rainbow trout integument requires a DNA locus involved in exopolysaccharide transport and biosynthesis. Environ Microbiol. 2007;9:370–82.

46. Zhu J, Mekalanos JJ. Quorum sensing-dependent biofilms enhance colonization in Vibrio cholerae. Dev Cell. 2003;5:647–56.
47. Milton DL, Toole R, Hörstedt P, Wolf-Watz H. Flagellin A is essential for the virulence of Vibrio anguillarum. J Bacteriol. 1996;178:1310.
48. Burmølle M, Hansen LH, Oregaard G, Sørensen SJ. Presence of N-acyl homoserine lactones in soil detected by a whole-cell biosensor and flow cytometry. Micro Ecol. 2003;45:226–36 https://doi.org/10.1007/s00248-002-2028-6.
49. Tan D, Gram L, Middelboe M. Vibriophages and their interactions with the fish pathogen Vibrio anguillarum. Appl Environ Microbiol. 2014;80:3128–40. http://aem.asm.org/content/80/10/3128.
50. Ceri H, Olson ME, Stremick C, Read RR, Morck D, Buret A. The Calgary Biofilm Device: new technology for rapid determination of antibiotic susceptibilities of bacterial biofilms. J Clin Microbiol. 1999;37:1771–6. http://www.ncbi.nlm.nih.gov/pubmed/10325322.
51. Ren D, Madsen JS, de la Cruz-Perera CI, Bergmark L, Sørensen SJ, Burmølle M. High-throughput screening of multispecies biofilm formation and quantitative PCR-based assessment of individual species proportions, useful for exploring interspecific bacterial interactions. Micro Ecol. 2014;68:146–54. https://doi.org/10.1007/s00248-013-0315-z.
52. Liu W, Russel J, Røder HL, Madsen JS, Burmølle M, Sørensen SJ. Low-abundant species facilitates specific spatial organization that promotes multispecies biofilm formation. Environ Microbiol. 2017;19:2893–905. http://www.ncbi.nlm.nih.gov/pubmed/27768826.
53. RStudio Team. RStudio: integrated development environment for R. Boston, MA: RStudio, Inc; 2016. http://www.rstudio.com/.
54. Luo TL, Eisenberg MC, Hayashi MAL, Gonzalez-Cabezas C, Foxman B, Marrs CF, et al. A sensitive thresholding method for confocal laser scanning microscope image stacks of microbial biofilms. Sci Rep. 2018;8:13013. https://doi.org/10.1038/s41598-018-31012-5.
55. Røder HL, Herschend J, Russel J, Andersen MF, Madsen JS, Sørensen SJ, et al. Enhanced bacterial mutualism through an evolved biofilm phenotype. ISME J. 2018;12:2608–18. https://doi.org/10.1038/s41396-018-0165-2.
56. Knowles B, Bailey B, Boling L, Breitbart M, Cobián-Güemes A, del Campo J, et al. Variability and host density independence in inductions-based estimates of environmental lysogeny. Nat Microbiol. 2017;2:17064. 10.1038/nmicrobiol.2017.64.
57. Weitz JS, Li G, Gulbudak H, Cortez MH, Whitaker RJ. Viral invasion fitness across a continuum from lysis to latency†. Virus Evol. 2019;5:1–9. https://doi.org/10.1093/ve/vez006/5476198.
58. Ball AS, Chaparian RR, van Kessel JC. Quorum sensing gene regulation by LuxR/HapR master regulators in Vibrios. Margolin W, editor. J Bacteriol. 2017;199:1–13. http://jb.asm.org/lookup/doi/10.1128/JB.00105-17.
59. Croxatto A, Pride J, Hardman A, Williams P, Cámara M, Milton DL. A distinctive dual-channel quorum-sensing system operates in Vibrio anguillarum. Mol Microbiol. 2004;52:1677–89.
60. Brum JR, Hurwitz BL, Schofield O, Ducklow HW, Sullivan MB. Seasonal time bombs: dominant temperate viruses affect Southern ocean microbial dynamics. ISME J. 2016;10:437–49. https://doi.org/10.1038/ismej.2015.125.
61. Igler C, Abedon ST. Commentary: A host-produced quorum-sensing autoinducer controls a phage lysis-lysogeny decision. Front Microbiol. 2019;10:1171. https://www.frontiersin.org/article/10.3389/fmicb.2019.01171/full.
62. Payet JP, Suttle CA. To kill or not to kill: the balance between lytic and lysogenic viral infection is driven by trophic status. Limnol Oceanogr. 2013;58:465–74.
63. Thompson FL, Iida T, Swings J. Biodiveristy of Vibrios. Microbiol Mol Biol Rev. 2004;68:403–31.
64. Kalatzis P, Castillo D, Katharios P, Middelboe M. Bacteriophage interactions with marine pathogenic Vibrios: implications for phage therapy. Antibiotics. 2018;7:15. http://www.mdpi.com/2079-6382/7/1/15.
65. Obeng N, Pratama AA, Elsas JDvan. The significance of mutualistic phages for bacterial ecology and evolution. Trends Microbiol. 2016;24:440–9. https://doi.org/10.1016/j.tim.2015.12.009.
66. Hansen MF, Svenningsen S Lo, Røder HL, Middelboe M, Burmølle M. Big impact of the tiny: bacteriophage–bacteria interactions in biofilms. Trends Microbiol. 2019;27:739–52. https://linkinghub.elsevier.com/retrieve/pii/S0966842X1930099X.
67. Fillol-Salom A, Alsaadi A, Sousa JAM de, Zhong L, Foster KR, Rocha EPC, et al. Bacteriophages benefit from generalized transduction. Otto M, editor. PLoS Pathog. 2019;15:e1007888. https://doi.org/10.1371/journal.ppat.1007888.
68. Argov T, Sapir SR, Pasechnek A, Azulay G, Stadnyuk O, Rabinovich L, et al. Coordination of cohabiting phage elements supports bacteria–phage cooperation. Nat Commun. 2019;10:5288.
69. Rice SA, Tan CH, Mikkelsen PJ, Kung V, Woo J, Tay M, et al. The biofilm life cycle and virulence of Pseudomonas aeruginosa are dependent on a filamentous prophage. ISME J. 2009;3:271–82.
70. Carrolo M, Frias MJ, Pinto FR, Melo-Cristino J, Ramirez M. Prophage spontaneous activation promotes DNA release enhancing biofilm formation in Streptococcus pneumoniae. PLoS ONE. 2010;5:e15678. http://www.pubmedcentral.nih.gov/articlerender.fcgi?artid=3004956&tool=pmcentrez&rendertype=abstract.
71. Gödeke J, Paul K, Lassak J, Thormann KM. Phage-induced lysis enhances biofilm formation in Shewanella oneidensis MR-1. ISME J. 2011;5:613–26. http://www.pubmedcentral.nih.gov/articlerender.fcgi?artid=3105746&tool=pmcentrez&rendertype=abstract.
72. Croxatto A, Chalker VJ, Lauritz J, Jass J, Hardman A, Williams P. et al. VanT, a homologue of Vibrio harveyi LuxR, regulates serine, metalloprotease, pigment, and biofilm production in Vibrio anguillarum. J Bacteriol. 2002;184:1617–29. https://doi.org/10.1128/jb.184.6.1617-1629.2002.
73. Hentzer M, Givskov M. Pharmacological inhibition of quorum sensing for the treatment of chronic bacterial infections. J Clin Invest. 2003;112:1300–7. http://www.jci.org/articles/view/20074.
74. O'Loughlin CT, Miller LC, Siryaporn A, Drescher K, Semmelhack MF, Bassler BL. A quorum-sensing inhibitor blocks Pseudomonas aeruginosa virulence and biofilm formation. Proc Natl Acad Sci USA. 2013;110:17981–6. http://www.ncbi.nlm.nih.gov/pubmed/24143808.
75. Shelford EJ, Middelboe M, Møller EF, Suttle CA. Virus-driven nitrogen cycling enhances phytoplankton growth. Aquat Micro Ecol. 2012;66:41–6.
76. Weitz JS, Stock CA, Wilhelm SW, Bourouiba L, Coleman ML, Buchan A, et al. A multitrophic model to quantify the effects of marine viruses on microbial food webs and ecosystem processes. ISME J. 2015;9:1352–64.
77. Zimmerman AE, Howard-Varona C, Needham DM, John SG, Worden AZ, Sullivan MB, et al. Metabolic and biogeochemical consequences of viral infection in aquatic ecosystems. Nat Rev Microbiol. 2019;18. https://doi.org/10.1038/s41579-019-0270-x.